Modulation of Skeletal Muscle Insulin Signaling With Chronic Caloric Restriction in Cynomolgus Monkeys

Zhong Q. Wang,[1] Z. Elizabeth Floyd,[1] Jianhua Qin,[1] Xiaotuan Liu,[1] Yongmei Yu,[1] Xian H. Zhang,[1] Janice D. Wagner,[2] and William T. Cefalu[1]

OBJECTIVE—Caloric restriction (CR) has been shown to retard aging processes, extend maximal life span, and consistently increase insulin action in experimental animals. The mechanism by which CR enhances insulin action, specifically in higher species, is not precisely known. We sought to examine insulin receptor signaling and transcriptional alterations in skeletal muscle of nonhuman primates subjected to CR over a 4-year period.

RESEARCH DESIGN AND METHODS—At baseline, 32 male adult cynomolgus monkeys (*Macaca fascicularis*) were randomized to an ad libitum (AL) diet or to 30% CR. Dietary intake, body weight, and insulin sensitivity were obtained at routine intervals over 4 years. At the end of the study, hyperinsulinemic-euglycemic clamps were performed and skeletal muscle (vastus lateralis) was obtained in the basal and insulin-stimulated states for insulin receptor signaling and gene expression profiling.

RESULTS—CR significantly increased whole-body insulin–mediated glucose disposal compared with AL diet and increased insulin receptor signaling, i.e., insulin receptor substrate (IRS)-1, insulin receptor phosphorylation, and IRS–associated PI 3-kinase activity in skeletal muscle ($P < 0.01$, $P < 0.01$, and $P < 0.01$, respectively). Gene expression for insulin signaling proteins, i.e., IRS-1 and IRS-2, were not increased with CR, although a significant increase in protein abundance was noted. Components of the ubiquitin-proteasome system, i.e., 20S and 19S proteasome subunit abundance and 20S proteasome activity, were significantly decreased by CR.

CONCLUSIONS—CR increases insulin sensitivity on a whole-body level and enhances insulin receptor signaling in this higher species. CR in cynomolgus monkeys may alter insulin signaling in vivo by modulating protein content of insulin receptor signaling proteins. ***Diabetes*** **58:1488–1498, 2009**

Caloric restriction (CR) can dramatically extend life span in lower species by retarding aging processes and reducing the incidence and severity of age-related diseases whether initiated in young or old age in mammalian models (1–5). Although longevity studies have not been completed in humans, it is well documented that lifestyle modification that includes CR can significantly delay progression and onset of type 2 diabetes. However, the cellular mechanism(s) by which CR exerts its effects on longevity and attenuates progression to metabolic diseases is not precisely known. CR has been postulated to reduce protein glycation and glycoxidation, scavenge reactive oxygen species, modulate thermogenesis, assist in DNA repair, and alter oncogene expression and protein degradation (5–10). Recently, sirtuin 1 (SIRT1) (one of the human homologues of the budding yeast Sir2) has been attracting great interest because of its role in the antiaging effects of CR (11,12).

With specific regard to the mechanism of action, studying the effects of CR on aging processes and age-related diseases in a long-lived nonhuman primate, particularly as it relates to the analysis of the genome, could provide greater insights into mechanisms of aging and effects on aging in humans. Although human studies have only recently been reported (13), there has been intense study of the metabolic effects of CR in higher species for many years. Specifically, we demonstrated that CR improved insulin sensitivity and reduced intra-abdominal fat with aging in a 4-year study in cynomolgus monkeys (14). An improvement in insulin sensitivity appears to be one of the most consistent features of CR, as observed in both rodent and nonhuman primate models (1–3,14–18). However, the cellular mechanism by which CR specifically enhances insulin action is not precisely known.

To evaluate the potential mechanism by which CR enhances insulin action would require investigation at multiple tissues in vivo because coordinated mechanisms from liver, adipocytes, and skeletal muscle all contribute to whole-body insulin action. Yet, analysis of skeletal muscle transcriptional regulation with CR would be an important step given that skeletal muscle is the major site of insulin-mediated glucose disposal. In addition, a major metabolic effect reported for insulin in muscle is inhibition of protein degradation, mediated by the ubiquitin-proteasome system (19,20). Interestingly, insulin resistance was also reported to accelerate proteasome-dependent degradation of muscle proteins (21), indicating that insulin signaling exerts control over proteasome function in skeletal muscle. Thus, we sought to determine a potential mechanism by which CR enhances insulin action in a higher species by evaluating insulin signaling and gene expression in skeletal muscle in a nonhuman primate subjected to chronic CR.

RESEARCH DESIGN AND METHODS

The effect of chronic CR to modulate cellular insulin signaling and transcriptional regulation was assessed in skeletal muscle obtained from nonhuman primates subjected to a 4-year period of 30% CR compared with ad libitum (AL) feeding conditions. The metabolic and physiological changes observed in this cohort with CR were previously reported (14). Specifically, 32 feral adult male cynomolgus monkeys (*Macaca fascicularis*) (mean ± SEM age 8.2 ± 1.2 years) were part of a randomized trial in which the independent effect of CR

From the [1]Division of Nutrition and Chronic Diseases, Pennington Biomedical Research Center, Louisiana State University System, Baton Rouge, Louisiana; and the [2]Department of Pathology, Wake Forest University School of Medicine, Winston-Salem, North Carolina.

Corresponding author: William T. Cefalu, william.cefalu@pbrc.edu.

Received 18 July 2008 and accepted 19 March 2009.

Published ahead of print at http://diabetes.diabetesjournals.org on 31 March 2009. DOI: 10.2337/db08-0977.

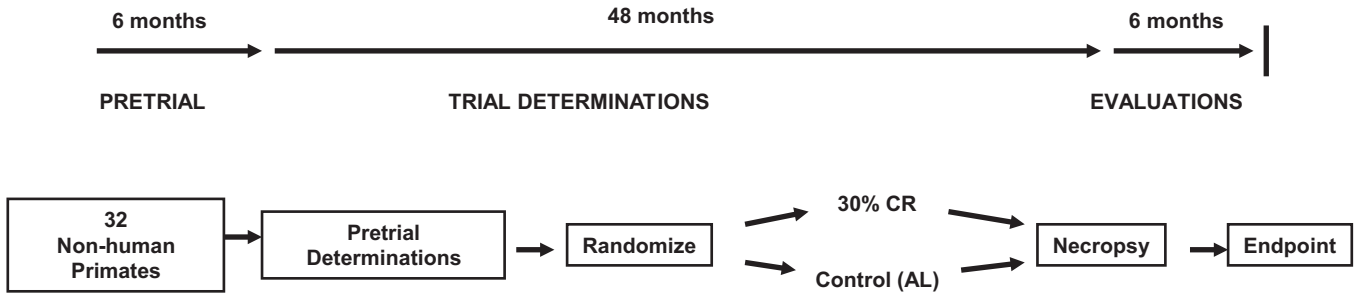

FIG. 1. Demonstration of the study design for the 4-year caloric restriction trial. As shown, after pretrial evaluations, the animals were randomly assigned to AL or CR diet (30%). After 48 months of intervention, clinical and cellular mechanisms were assessed.

and its interaction with insulin resistance and atherosclerotic lesion extent and composition were evaluated (Fig. 1).

The animals were acquired directly from the Institute Pertanian (Bogar, Indonesia) and quarantined for 3 months. Animals were housed socially in pairs except when separated at mealtime by sliding a partition to separate them (14). Beginning in the 4th month and throughout the pretrial (months 4–6), all animals were fed a moderately atherogenic diet (0.25 mg cholesterol/calorie) containing 30% of calories from fat. Caloric intake for each animal was assessed by feeding a known allotment and weighing the uneaten food (14). After pretrial evaluations, the animals were assigned to AL or CR diet groups using a stratified randomization. The CR diet was introduced over a 3-month transition period (90% of AL intake during the 1st month, 80% during the 2nd month, and 70% during the 3rd month and thereafter). Additional vitamin and mineral mixture, β-sitosterol, and crystalline cholesterol were added to the CR diet so that the same amount of these components was ingested regardless of the randomized group (14).

Insulin sensitivity. Insulin sensitivity was assessed at 6-month intervals using a modified minimal model and at the end of the study using a hyperinsulinemic-euglycemic clamp as described (14). At the baseline of the clamp, a biopsy of the vastus lateralis muscle was obtained. After the insulin infusion, repeat biopsies were obtained at 5, 20, and 40 min of the clamp. Muscle samples (~200 mg wet wt) were immediately placed into liquid nitrogen and then stored at −80°C. There was no difference between the steady state plasma glucose (5.38 ± 0.10 vs. 5.42 ± 0.10 mmol/l) or plasma insulin levels observed during the clamp (1,472 ± 145 vs. 1,535 ± 155 pmol/l) for either the CR or AL groups, respectively.

Tissue preparation. Muscle tissue lysates were prepared by dissection and homogenized in buffer A (25 mmol/l HEPES, pH 7.4, 1% Nonidet P-40, 137 mmol/l NaCl, 1 mmol/l phenylmethylsulfonyl fluoride, 10 μg/ml aprotinin, 1 μg/ml pepstatin, and 5 μg/ml leupeptin), using a PRO 200 homogenizer (PRO Scientific, Oxford, CT). The samples were centrifuged at 14,000*g* for 20 min at 4°C, and protein content of the supernatant was determined (Bio-Rad protein assay kit; Bio-Rad Laboratories, Hercules, CA). Supernatants (50 μg) were resolved by SDS-PAGE and subjected to immunoblotting using chemiluminescence reagent (PerkinElmer Life Science, Boston, MA) and quantified as described (22). The 19S proteasome base anti-S5A/Rpn10 antibodies were ordered from Calbiochem (Gibbstown, NJ). Antibodies for phospho–insulin receptor substrate (IRS)-1 (Tyr612), phospho–insulin receptor (IR) (Tyr1150/1151), phosphoinositol (PI) 3-kinase protein 85 (p85 of PI 3-kinase), phospho-Akt (Ser473), IRS-1 and IRS-2, 20S proteasome subunit β2i, Akt, serum- and glucocorticoid-inducible kinase 1 (SGK1), signal transducer and activator of transcription 3 (STAT3), and SIRT1 antibodies were obtained from Upstate Biotech (Lake Placid, NY). Anti-19S proteasome lid subunits S9/Rpn6 and S14/Rpn12 antibodies were ordered from BIOMOL International (Plymouth Meeting, PA). GLUT4 monoclonal antibody was obtained from R&D Systems (Minneapolis, MN). Lipoprotein lipase (LPL) antibody was purchased from GeneTex (San Antonio, TX) and β-actin from Affinity Bioreagents (Golden, CO). IR β-subunit was obtained from Santa Cruz Biotechnology (Santa Cruz, CA).

IR tyrosine kinase activity. IR tyrosine kinase activity was assessed as described by Le Marchand-Brustel et al. (23) with modification. Briefly, 500 μg of muscle lysate at each time point was added to 50 μl of agarose bound wheat germ agglutinin incubated at room temperature for 2 h. After washing with buffer A, bound receptor was eluted by 3 mol/l *N*-acetyl-D-glucosamine solution. IR kinase activity was initialed by adding 40 μl of reaction solution consisting of 1 mmol/l DTT, 10 mmol/l $MgCl_2$, 3 mmol/l $MnCl_2$, and 5 μmol/l [r-^{32}P]ATP. Reactions were carried out for 30 min at 22°C and terminated by adding 2 μl of 0.5 mol/l EDTA and 10 μl of 500 μmol/l ATP. Then 2 μg of IR β-subunit antibody and 50 μl of protein A agarose beads were added to the reaction mixture and incubated at room temperature for 30 min. After extensive washing with buffer A, 40 μl of electrophoresis sample buffer was added and heated at 95°C for 4 min. Following SDS-PAGE, gels were dried and bands visualized by autoradiography.

IR β-subunit tyrosine phosphorylation. IR β-subunit tyrosine phosphorylation and IR β-subunit abundance were measured by Western blot techniques (24,25). Briefly, 50 μg of lysates prepared as described above was subjected to 8% SDS-PAGE and transferred to nitrocellulose membrane. IR β-subunit phosphorylation was detected with anti–phospho-IR (Tyr1150/1151) antibody. The membrane was striped with strip buffer and reprobed with anti–IR β-subunit and β-actin antibodies, respectively.

Insulin-stimulated tyrosine phosphorylation of IRS-1, PI 3-kinase activity, and Akt phosphorylation. To assess IRS-1 phosphorylation, muscle lysates were subjected to SDS-PAGE (24). The bands were detected with anti–phospho-IRS-1 (Tyr612) antibody (26). After measuring phospho-IRS-1 abundance, the membrane was striped with strip buffer and reprobed with anti–total IRS-1 antibody to obtain abundance. IRS-1–associated PI 3-kinase activities of the muscle at each time point were assessed (25–27). We confirm that wortmannin treatment could completely inhibit IRS-1–associated PI 3-kinase activity of muscle tissues (data not shown). Total Akt and pAkt (Ser473) at each time point were similarly assessed with Western blot techniques.

Protein content for IRS-2, GLUT4, PI 3-kinase (p85), LPL, SGK1, SIRT1, and STAT3 in the lysates was measured also using Western blot analysis. Results of scanning for each gel were normalized by β-actin, and the data are presented as mean ± SEM of fold change in CR versus AL.

RNA extraction. Total RNA was extracted from muscle obtained for microarray and real-time quantitative PCR (qPCR) assays. Frozen tissues were placed in a mortar in liquid nitrogen, and the tissue was pulverized into powder using a pestle on dry ice. Total RNA was isolated from the tissue powder using TRIZOL reagent (Invitrogen, Carlsbad, CA). After DNase I (Invitrogen) digestion, RNA was further purified with an RNeasy Mini Kit (QIAGEN, Germantown, MD). RNA concentration and quality were measured by an RNA 6000 Nano LabChip kit (Agilent Technologies, Santa Clara, CA).

Gene expression. The Applied Biosystems human genome survey microarray version 2.0 chip containing 32,878 oligonucleotide probes (60-mer) representing 29,098 individual human genes and more than 1,000 control probes was used for microarray profiling for 10 animals, 5 randomly chosen from each group. It has been demonstrated that human sequence–based DNA arrays can be used effectively to detect differential gene expression in a nonhuman primate (28). Digoxigenin-UTP–labeled cRNA was generated and linearly amplified from 1 μg of total RNA from each sample using an Applied Biosystems Chemiluminescent RT-IVT labeling kit according to the manufacturer's protocol. After cRNA was fragmented by heating at 60°C for 30 min, 10 μg of cRNA fragments were hybridized at 55°C for 16 h. Chemiluminescence detection, image acquisition, and analysis were performed according to the manufacturer's protocol (Applied Biosystems, Foster, CA). Signals were quantified and corrected for background, and final images and feature data were processed by Applied Biosystems 1700 Chemiluminescent Microarray Analyzer software version 1.1.

Real-time qPCR. The primer sequences of candidate genes were designed using Primer Express software version 3.0 (Applied Biosystems). A 1-μg aliquot of total RNA for each sample was reverse transcribed in a 100-μl reaction volume with a commercial High-Capacity cDNA Archive Kit (Applied Biosystems) according to the manufacturer's protocol. The qPCR was conducted in 384-well microtiter plates on the ABI Prism Sequence Detector 7900 (Applied Biosystems) with Bio-Rad iTaqTM SYBR Green Supermix with ROX Kits. For each sample of each gene, PCR amplification was performed in triplicate with β-actin used as an endogenous control. The mRNA content of each candidate gene was determined simultaneously in 10 paired (CR and AL)

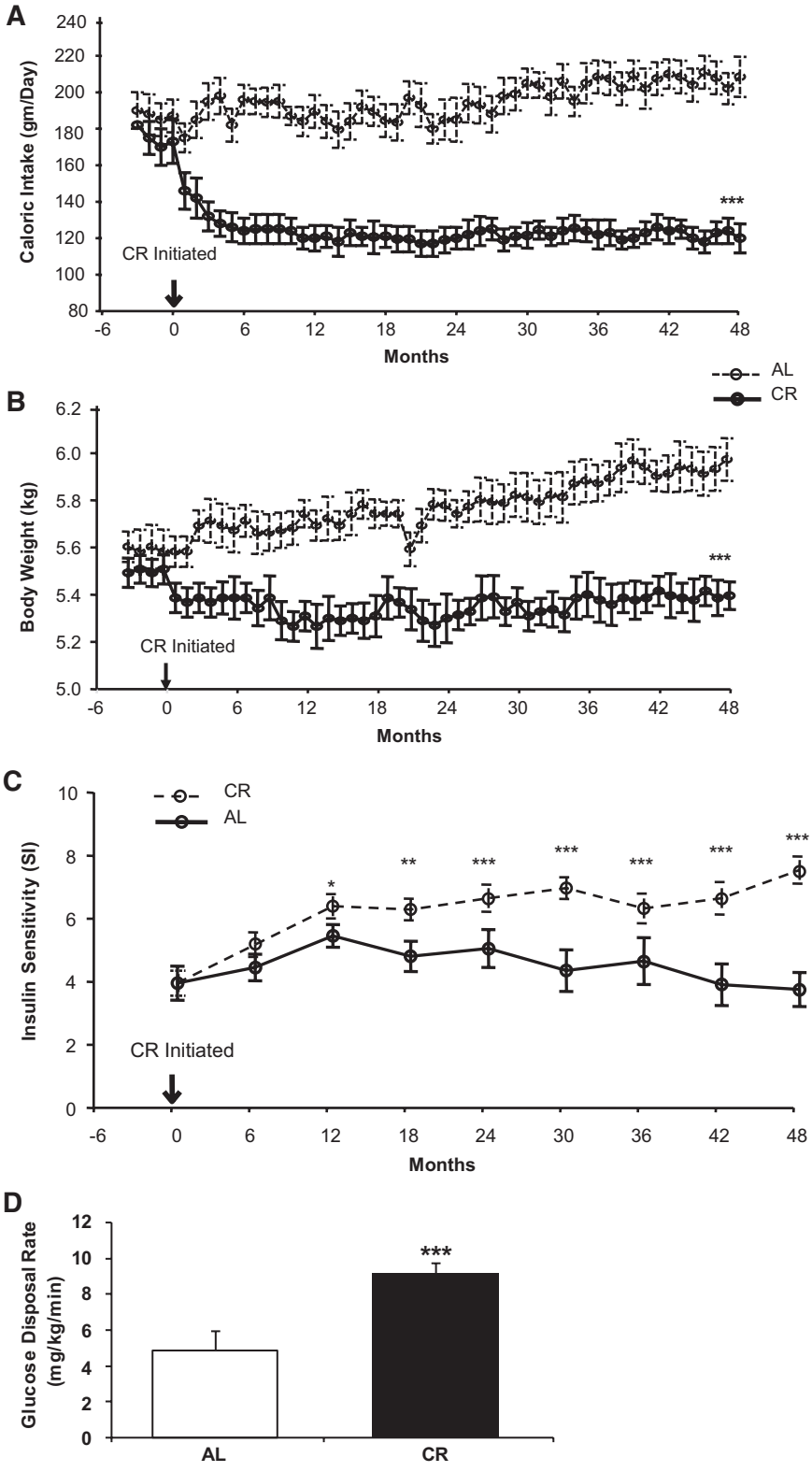

FIG. 2. Caloric intake (*A*) and body weight (*B*) for both treatment groups over 4 years of observations are demonstrated. *C* demonstrates results of insulin sensitivity assessed every 6 months over the course of study, using the minimal model technique. *D* demonstrates insulin sensitivity assessed by hyperinsulinemic-euglycemic clamps conducted at the end of the study. Data are means ± SEM (n = 16 per group). SI units = $10^{-4} \cdot \text{min}^{-1} \cdot \mu\text{U}^{-1} \cdot \text{ml}$. *$P < 0.05$, **$P < 0.01$, and ***$P < 0.001$ for CR versus AL. (All data presented in this figure have been previously published, and the figure was modified from Cefalu et al. [14] with permission.)

muscle samples assessed by DNA array analysis. The assay was performed in duplicate.

20S proteasome activity assay. 20S proteasome activity in muscle lysates obtained in the basal state was measured in duplicate using a 20S Proteasome Activity Assay Kit (Chemicon International, Temecula, CA). 20S proteasome chymotrypsin activity was measured by incubating 20 μg of each lysate with fluorophore 7-amino-4-methylcoumarin (AMC)-labeled peptide substrate LLVY-AMC at 37°C for 60 min. The free AMC released by proteasome activity

was quantified using a 380/460-nm filter set in a fluorometer (BioTex, Winooski, VT). The AMC standard curve was generated with a series dilution of AMC standard solution. Proteasome activity was confirmed using purified 20S proteasome as the positive control and is reported as μmol/l AMC per mg protein per h. Each sample/substrate combination was measured both in the presence and in the absence of MG132 (10 μmol/l) or epoxomicin (1 μmol/l), a highly specific 20S proteasome inhibitor (Boston Biochem, Cambridge, MA) (29), to account for any nonproteasomal degradation of the substrate.

Statistical analysis. The effects of CR on the trial evaluations measured at the specified intervals postrandomization were estimated using repeated-measures ANCOVA. Analysis of group differences was adjusted for the prerandomization levels of the outcome measure tested in order to reduce the variance explained by prerandomization predictors. All tests of hypotheses and reported *P* values were two-sided. Whenever a baseline value was used as a covariate in an ANCOVA model, an interaction term between the group and the covariate was initially included to check the parallelism assumption. If the interaction was not significant at the 0.10 level of significance, and it was always the case, the interaction term was omitted.

For gene expression, within-array normalization was done with the scanning software from Applied Biosystems based on housekeeping genes on each array. Global normalization among arrays was accomplished using quantile normalization (30). ANOVA analysis with Bonferroni adjustment was used for detecting significantly differentiated genes. Differentially expressed genes between the CR and AL groups were determined based on the following criteria: Bonferroni-adjusted $P < 0.05$ and fold change in the CR over the AL group of ≥1.5. All data analyses were carried out using SAS (Cary, NC). Public databases including David/Ease, GenMAPP, Panther, GOTM, and TreeView version 1.6 were used to assess functional gene cluster analysis (31).

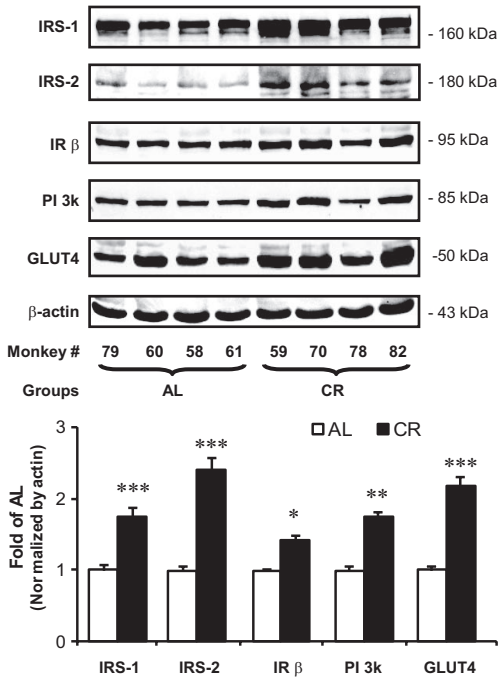

FIG. 3. Content of insulin receptor signaling proteins in the monkey skeletal muscle obtained at basal state is demonstrated. IRS-1, IRS-2, IR β-subunit, PI 3-kinase (p85), and GLUT4 protein abundance in the muscle were measured by Western blot analysis. Results were normalized by β-actin level. Data are means ± SEM (n = 13 per group) as fold change of AL at baseline. *$P < 0.05$, **$P < 0.01$, and ***$P < 0.001$ for CR versus AL.

RESULTS

The clinical, phenotypic, and metabolic effects of CR for the cohort of cynomolgus monkeys (*Macaca fascicularis*) evaluated were previously reported in detail (14). Compared with the AL group, animals randomized to CR were observed to have significantly reduced dietary intake, reduced body weight, increased insulin sensitivity, and reduced intra-abdominal fat with aging (Fig. 2*A*–*D*) (14). The effect of CR was noted during the 1st year of observation and maintained over the 4 years of observation, as demonstrated not only from periodic assessment of insulin sensitivity with the minimal model (Fig. 2*C*), but also from the assessment with hyperinsulinemic-euglycemic clamps obtained at study end (Fig. 2*D*) (14).

Insulin signaling. Animals randomized to CR had significantly increased skeletal muscle protein abundance of IRS-1, IRS-2, IR β-subunit, PI 3-kinase (p85), and GLUT4 compared with that in the AL group (Fig. 3). When compared with AL animals, animals randomized to CR had enhanced insulin-stimulated skeletal muscle IR tyrosine kinase activity (data not shown) and increased IR β-subunit phosphorylation (Fig. 4*A*) and IRS-1 phosphorylation (Fig. 4*B*). IRS-1 protein levels measured at the 5-, 20-, and 40-min time points did not differ from the value assessed as the 0 time point. Although there was no significant difference in basal PI 3-kinase activity between the CR and AL groups, insulin-stimulated PI 3-kinase activities were significantly higher when assessed at all time points post–insulin stimulation in the CR group compared with those in the AL group (Fig. 4*C*). Akt phosphorylation post–insulin stimulation was also increased in skeletal muscle with CR when compared with AL (Fig. 4*D*).

Genomic analysis. A total of 241 genes were identified as significantly differentially expressed with CR from 10,163 probes with a satisfactory quality of signals over all the array slides. Among them, 179 genes were observed to be downregulated and 62 genes upregulated. Using cluster analysis, gene expression differed in 11 categories of biological processes with ~18% of genes involved in either carbohydrate and lipid metabolism or signal transduction (Fig. 5). Tables 1 and 2 list genes of interest in the muscle that were either significantly upregulated or downregulated with CR for each biological process, respectively.

To confirm the microarray findings, real-time qPCR assays were conducted. Altogether, 27 genes were selected from the microarray analysis to measure transcription levels using RT-qPCR for which 22 were confirmed to have significant changes in the CR compared with the AL group (Table 3). Two genes, i.e., STAT3 and interleukin 6 signal transducer (IL6ST), did not show significant changes between AL and CR conditions as assessed with real-time qPCR assays as opposed to the microarray analysis, and expression of the type 3 iodothyronine deiodinase (*DIO3*) gene with RT-qPCR did not agree with the findings from the microarray. In addition, SIRT1 transcriptional level in muscle from the CR monkeys was significantly increased compared with that from the AL monkeys, as assessed by RT-qPCR assay.

From the list of genes confirmed by RT-qPCR, LPL, SGK1, SIRT1, and STAT3 were assessed for protein abundance (Fig. 6). The protein abundance of LPL, SGK1, and SIRT1 was significantly increased in the CR compared with the AL group (97, 57, and 35%, respectively). In agreement with the PCR data, protein expression of STAT3 in the CR monkeys was not confirmed by Western blot analysis (Fig. 6). Because increased gene expression of insulin signaling proteins (i.e., IRS-1, IRS-2, and PI 3-kinase) was not noted, yet increased protein content was observed, factors that regulate protein content (i.e., degradation) were sought. The majority of intracellular proteins are degraded by the 26S proteasome (32). Given the inhibitory effect of

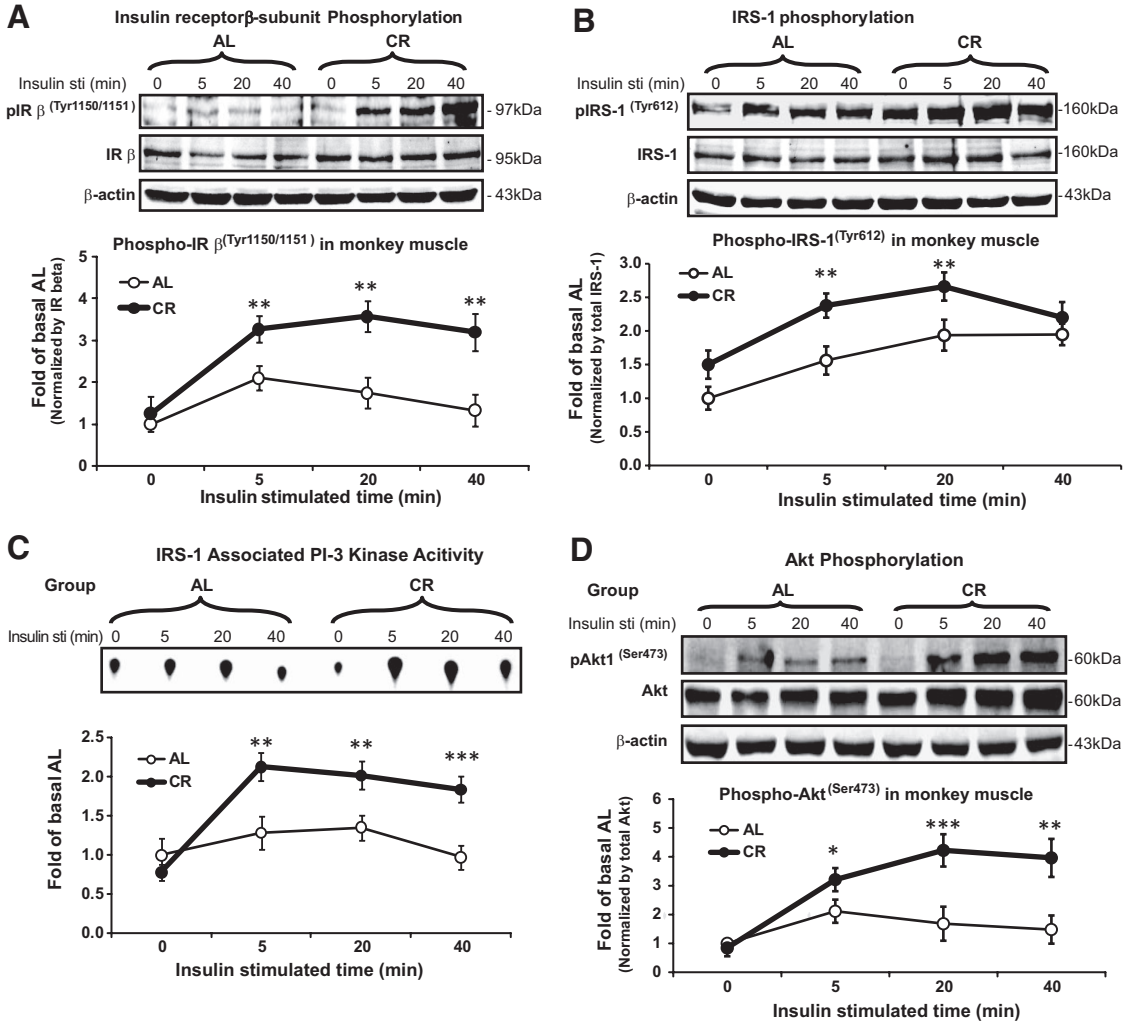

FIG. 4. IR β-subunit phosphorylation (*A*), IRS-1 phosphorylation (*B*), IRS-1–associated PI 3-kinase activities (*C*), and total Akt and pAkt (Ser473) (*D*) in the muscles at baseline (0 time point) and at 5, 20, and 40 min post–insulin stimulation are demonstrated. Data are means ± SEM (n = 6 per group). *P < 0.05, **P < 0.01, and ***P < 0.001 for CR versus AL.

insulin reported for proteasome-dependent protein degradation (19,20), 20S proteasome activity was assayed in the monkey muscle lysates. 20S proteasome activity in muscle lysates was significantly reduced in the CR group compared with the AL group, although nonproteasomal degradation measured in the presence of two

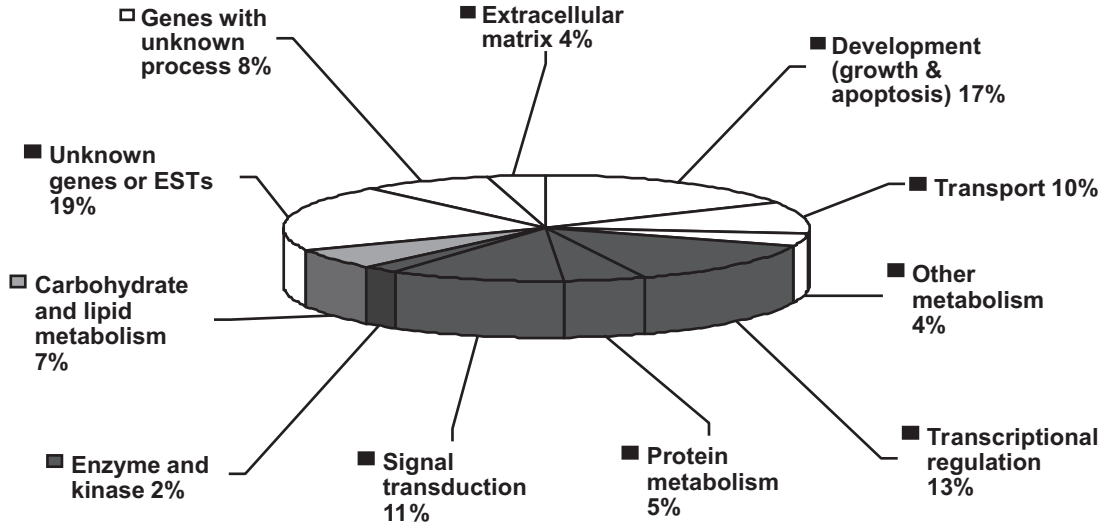

FIG. 5. Percentage of 241 genes modulated by CR and sorted by biological process for which fold-change was ≥1.5 and P was <0.05 (n = 5 per group).

TABLE 1
Genes observed to be upregulated by CR

Accession	Symbol	Fold-change	Gene name
Carbohydrate and lipid metabolism			
NM_018677	*ACSS2*	1.53	Acyl-CoA synthetase short-chain family member 2
NM_001647	*APOD*	2.45	Apolipoprotein D
NM_000237	*LPL*	1.99	Lipoprotein lipase
NM_003706	*PLA2G4C*	2.73	Phospholipase A2, group IVC
NM_020422	*LOC57146*	2.60	Promethin
NM_022479	*WBSCR17*	1.69	Williams-Beuren syndrome chromosome region 17
Development (growth, cell cycle, and apoptosis)			
NM_022662	*ANAPC1 RGPD1*	1.52	Anaphase promoting complex subunit
NM_001798	*CDK2*	1.72	Cyclin-dependent kinase 2
NM_030588	*DHX9*	1.70	DEAH (Asp-Glu-Ala-His) box polypeptide 9
NM_004426	*PHC1*	1.56	Polyhomeotic-like 1
NM_001004125	*TUSC1*	1.55	Tumor suppressor candidate 1
NM_001077397	*IRF2BP2*	1.53	Interferon regulatory factor 2 binding protein 2
Other metabolism			
NM_001003800	*BICD2*	1.51	Bicaudal D homolog 2 (*Drosophila*)
NM_003875	*GMPS*	1.63	Guanine monophosphate synthetase
NM_004813	*PEX16*	1.99	Peroxisomal biogenesis factor 16
NM_018663	*PXMP2*	1.88	Peroxisomal membrane protein 2, 22 kDa
Protein biosynthesis, metabolism, and catabolism			
NM_001010853	*ACY1L2*	1.93	Aminoacylase 1-like 2
NM_001414	*EIF2B1*	1.51	Eukaryotic translation initiation factor 2B, subunit 1
NM_176792	*MRPL43*	1.51	Mitochondrial ribosomal protein L43
NM_005401	*PTPN14*	1.64	Protein tyrosine phosphatase, non-receptor type 14
XM_114317	*RPL22L1*	1.90	Ribosomal protein L22-like 1
NM_005617	*RPS14*	2.42	Ribosomal protein S14
Signal transduction			
NM_199327	*SPRY1*	1.51	Sprouty homolog 1, antagonist of FGF signaling
NM_000627	*LTBP1*	2.06	Latent transforming growth factor β binding protein 1
NM_001388	*DRG2*	1.56	Developmentally regulated GTP binding protein 2
NM_002184	*IL6ST*	1.62	Interleukin 6 signal transducer
NM_004887	*CXCL14*	2.88	Chemokine (C-X-C motif) ligand 14
NM_003150	*STAT3*	1.51	Signal transducer and activator of transcription 3
NM_021183	*RAP2C*	1.55	RAP2C, member of RAS oncogene family
Transcriptional regulation			
NM_005316	*GTF2H1*	1.87	General transcription factor IIH
NM_006559	*KHDRBS1*	1.56	KH domain containing, RNA binding
NM_016199	*LSM7*	1.97	LSM7 homolog, U6 small nuclear RNA associated
NM_005120	*MED12*	1.56	Mediator of RNA polymerase II transcription
NM_002582	*PARN*	1.56	Poly(A)-specific ribonuclease
NM_006468	*POLR3C*	1.98	Polymerase (RNA) III polypeptide C (62 kD)
NM_006022	*TSC22D1*	1.69	TSC22 domain family, member 1
NM_004814	*WDR57*	1.51	WD repeat domain 57 (U5 snRNP specific)
NM_004773	*ZNHIT3*	1.63	Zinc finger, HIT type 3
Transport			
NM_198098	*AQP1*	2.08	Aquaporin 1
NM_001650	*AQP4*	1.93	Aquaporin 4
NM_001752	*CAT*	1.73	Catalase
NM_000747	*CHRNB1*	1.54	Cholinergic receptor, β polypeptide 1 (muscle)
NM_003665	*FCN3*	2.21	Ficolin (collagen/fibrinogen domain containing) 3
NM_001038618	*NARF*	1.51	Nuclear prelamin A recognition factor
NM_021977	*SLC22A3*	2.21	Solute carrier family 22, member 3
NM_016930	*STX18*	1.54	Syntaxin 18

independent proteasome inhibitors, i.e., MG132 or epoxomicin, was unchanged (Fig. 7*A*). Decreased 20S proteasome activity with CR was associated with significantly decreased abundance of selected subunits of the 26S proteasome, including a subunit of the 20S catalytic core (β2i) and subunits of the 19S regulatory complex base (S5A, which contains a ubiquitin binding site) and lid (Rpn6 and Rpn12, two of eight non-ATPase subunits) (Fig. 7*B* and *C*), when compared with the AL group.

DISCUSSION

One of the most consistent physiological changes observed with CR is the favorable effect on glucoregulation,

TABLE 2
Genes downregulated by CR

Accession	Symbol	Fold change	Gene name
Apoptosis			
NM_023067	*FOXL2*	−1.70	Forkhead box L2
NM_006054	*RTN3*	−1.60	Reticulon 3
NM_182985	*RNF36*	−1.60	Ring finger protein 36
Carbohydrate and lipid metabolism			
NM_006212	*PFKFB2*	−1.67	6-phosphofructo-2-kinase/fructose-2
NM_001607	*ACAA1*	−2.40	Acetyl-coenzyme A acyltransferase 1
NM_017990	*PDPR*	−1.50	Pyruvate dehydrogenase phosphatase regulatory
NM_014474	*SMPDL3B*	−1.68	Sphingomyelin phosphodiesterase, acid-like 3B
Development (growth and cell cycle)			
NM_004924	*ACTN4*	−1.51	Actinin, α4
NM_003741	*CHRD*	−1.69	Chordin
NM_001362	*DIO3*	−2.42	Deiodinase, iodothyronine, type III
NR_002770	*DIO3OS*	−1.72	Deiodinase, iodothyronine, type III opposite strand
NM_019612	*IRGC*	−2.62	Immunity-related GTPase family, cinema
NM_181602	*KRTAP6-1*	−1.80	Keratin associated protein 6-1
NM_005018	*PDCD1*	−1.52	Programmed cell death 1
NM_152362	*TNFAIP8L1*	−1.83	Tumor necrosis factor-α–induced protein 8-like 1
Extracellular matrix			
NM_152462	*AMAC1*	−1.70	Acyl-malonyl condensing enzyme 1
NM_001625	*AK2*	−2.61	Adenylate kinase 2
NM_001630	*ANXA8*	−1.65	Annexin A8
NM_004933	*CDH15*	−1.86	Cadherin 15, M-cadherin (myotubule)
NM_000632	*ITGAM*	−1.89	Integrin, αM
Protein biosynthesis, metabolism, and catabolism			
NM_007272	*CTRC*	−1.52	Chymotrypsin C (caldecrin)
NM_031948	*PRSS27*	−1.70	Protease, serine 27
NM_001001	*RPL36AL*	−2.08	Ribosomal protein L36a-like
NM_171997	*USP2*	−1.64	Ubiquitin specific peptidase 2
NM_017414	*USP18*	−1.99	Ubiquitin specific peptidase 18
Signal transduction			
NM_000054	*AVPR2*	−1.92	Arginine vasopressin receptor 2
NM_005283	*XCR1*	−1.86	Chemokine (C motif) receptor 1
NM_015722	*DRD1IP*	−1.53	Dopamine receptor D1 interacting protein
NM_005301	*GPR35*	−1.62	G protein–coupled receptor 35
NM_018485	*GPR77*	−1.66	G protein–coupled receptor 77
NM_020400	*GPR92*	−1.73	G protein–coupled receptor 92
NM_020988	*GNAO1*	−1.56	Guanine nucleotide binding protein (G protein)
NM_005340	*HINT1*	−2.74	Histidine triad nucleotide binding protein 1
NM_000894	*LHB*	−1.52	Luteinizing hormone β polypeptide
NM_004160	*PYY*	−2.15	Peptide YY
NM_004248	*PRLHR*	−1.98	Prolactin releasing hormone receptor
Transcriptional regulation			
NM_006161	*NEUROG1*	−1.76	Neurogenin 1
NM_024019	*NEUROG2*	−1.66	Neurogenin 2
NM_006231	*POLE*	−1.53	Polymerase (DNA directed), epsilon
NM_138338	*POLR3H*	−1.81	Polymerase (RNA) III (DNA directed) polypeptide H
NM_003317	*TITF1*	−1.68	Thyroid transcription factor 1
NM_152600	*ZNF579*	−1.62	Zinc finger protein 579
Transport			
NM_006028	*HTR3B*	−2.21	5-hydroxytryptamine (serotonin) receptor 3B
NM_138813	*ATP8B3*	−2.66	ATPase, class I, type 8B, member 3
NM_013387	*UCRC*	−2.73	Ubiquinol–cytochrome c reductase complex
NM_020443	*NAV1*	−1.95	Neuron navigator 1
NM_020822	*KCNT1*	−1.68	Potassium channel, subfamily T, member 1
NM_001038	*SCNN1A*	−2.44	Sodium channel, nonvoltage-gated 1α
NM_019025	*SMOX*	−1.65	Spermine oxidase
NM_003374	*VDAC1*	−1.56	Voltage-dependent anion channel 1

i.e., increased insulin sensitivity, as reported for both rhesus monkeys and rodents (1–3,15–17). Our data confirm that CR markedly improved insulin sensitivity in cynomolgus monkeys when evaluated over a 4-year period (14). In addition, we provide novel data regarding the cellular mechanism of action of CR because the enhanced

TABLE 3
Genes confirmed by RT-qPCR in skeletal muscle

Accession	Symbol	Gene name	Microarray mean Fold-change (CR/AL)	Microarray mean *P*	qPCR mean Fold-change (CR/AL)	qPCR mean *P*
Carbohydrate and lipid metabolism						
NM_000237	*LPL*	Lipoprotein lipase	+1.97	0.03	+2.37	0.009
NM_006212	*PFKFB2*	6-phosphofructo-2-kinase/fructose-2,6-biphosphatase 2	+1.71	0.02	+1.79	0.005
NM_003706	*PLA2G4C*	Phospholipase A2, group IVC (cytosolic, calcium-independent)	+2.72	0.01	+2.46	0.019
NR_002168	*PPP1R2P3*	Protein phosphatase 1, regulatory subunit 2 pseudogene 3	−2.5	0.03	−1.42	0.006
Development (growth, apoptosis, and cell cycle)						
NM_000618	*IGF1*	Insulin-like growth factor 1	+1.96	0.03	+1.65	0.05
NM_000597	*IGFBP2*	Insulin-like growth factor binding protein 2, 36 kDa	+1.95	0.01	+1.88	0.002
Genes with unknown process						
NM_182972	*IRF2BP2*	Interferon regulatory factor 2 binding protein 2	+1.50	0.01	+1.60	0.002
Other process						
NM_012238.3	*SIRT1*	Sirtuin 1	1.00	0.98	+2.03	0.01
NM_001752	*CAT*	Catalase	+1.73	0.03	+1.8	0.05
NM_001362	*DIO3*	Deiodinase, iodothyronine, type III	−2.4	0.02	+2.56	0.006
Protein metabolism						
NM_005627	*SGK1*	Serum/glucocorticoid regulated kinase 1	+1.71	0.001	+1.52	0.05
NM_017414	*USP18*	Ubiquitin specific peptidase 18	−1.99	0.002	−4.14	0.001
Signal transduction						
NM_001388	*DRG2*	Developmentally regulated GTP binding protein 2	+1.6	0.04	+2.93	0.05
NM_002184	*IL6ST*	Interleukin 6 signal transducer	+1.6	0.02	+1.38	0.09
NM_005544	*IRS1*	Insulin receptor substrate 1	1.04	0.84	−1.11	0.76
NM_003749	*IRS2*	Insulin receptor substrate 2	−1.04	0.82	1.36	0.15
NM_000208	*INSR*	Insulin receptor	1.36	0.06	1.81	0.01
NM_181504	*PIK3R1*	PI 3-kinase, regulatory subunit 1 (p85 α)	1.19	0.47	−1.25	0.1
NM_001042	*SLC2A4*	Glucose transporter 4	1.43	0.04	3.35	0.01
Transcriptional regulation						
NM_001357	*DHX9*	DEAH (Asp-Glu-Ala-His) box polypeptide 9	+1.80	0.04	+1.89	0.001
NM_023067	*FOXL2*	Forkhead box L2	−1.7	0.01	−1.59	0.05
NM_003150	*STAT3*	Signal transducer and activator of transcription 3	+1.5	0.01	+1.36	0.28
Transportation						
NM_198098	*AQP1*	Aquaporin 1	+2.08	0.04	+3.38	0.001
NM_182964	*NAV2*	Neuron navigator 2	−1.6	0.02	−2.17	0.03
NM_006054	*RTN3*	Reticulon 3	−1.6	0.002	−1.96	0.004
NM_013387	*UCRC*	Ubiquinol–cytochrome c reductase complex 7.2 kDa protein	−2.7	0.004	−2.17	0.005
Unknown genes						
NM_020422	*TMEM159*	Transmembrane protein 159	+2.70	0.04	+1.44	0.03

insulin action observed in animals randomized to CR, as opposed to AL, was associated with increased content of proteins of the IR signal transduction pathway.

Enhanced insulin signaling was demonstrated in our study with the finding of increases in IR kinase activities, IR β-subunit phosphorylation, and IRS-1–associated PI 3-kinase activities following insulin stimulation in the muscle tissues in the CR group. The mechanism by which insulin signaling is enhanced with CR has been suggested to be secondary to an effect on transcriptional regulation. For example, it has been reported that liver IR, IGF-1R, and IRS-1 mRNA were greater in older rats subjected to 25 months of 40% CR than in AL-fed rats (33) and that CR also had greater effect on the cardiac gene expression of IR, IRS-1, IGF-1, IGF-1R, and GLUT4 compared with that in age-matched controls (34). In contrast, studies reported for primates subjected to CR do not support the observations in rodents as related to transcription. Kayo et al. (35) evaluated skeletal muscle from rhesus monkeys subjected to CR and reported increases in gene expression of GLUT4, which agree with our data. Moreover, they also reported increased gene expression of PI 3-kinase P110,

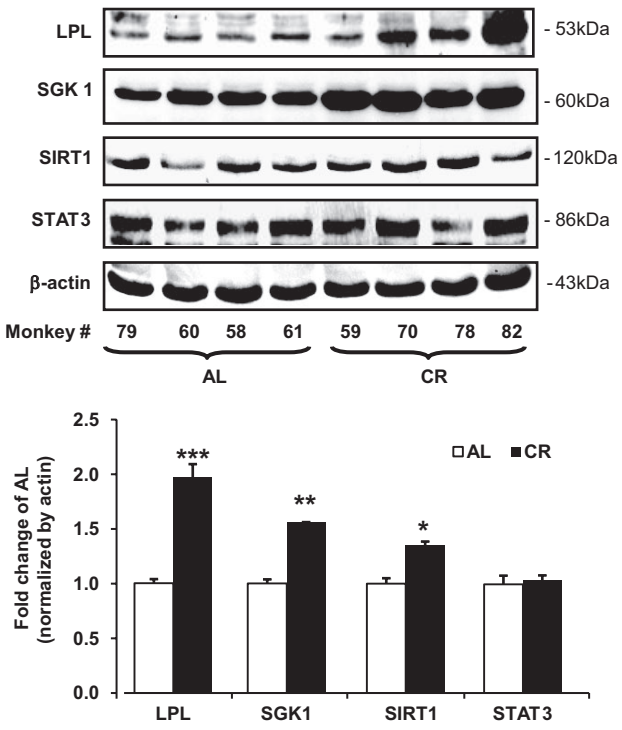

FIG. 6. Protein content for LPL, SGK1, SIRT1, and STAT3 in the muscle tissues obtained at the basal time point. Data were normalized by β-actin and expressed as fold change of AL. Data are means ± SEM (n = 13 per group). *P < 0.05, **P < 0.01, ***P < 0.001 for CR versus AL.

β-isoform. There were clear differences in our study compared with the other reported studies in that we evaluated a different primate species (i.e., cynomolgus vs. rhesus monkeys), a different dietary content (i.e., atherogenic diet vs. chow), and a later start date for initiation of CR (14–18,35).

Given our observations, the major question would be the mechanism by which insulin signaling protein content in muscle is increased without a significant effect on transcriptional regulation. Ambient protein levels are determined by the coordinated interplay of metabolic processes that involve transcription, mRNA translation, and degradation (36). Transcription and degradation mechanisms have received significant attention, and regulation at the level of mRNA translation as an independent mechanism is suggested when mRNA and protein levels do not correlate (36). It is also reported that the content of IRS-1 and IRS-2 is influenced by many factors, including growth factors and cytokines, and conditions associated with insulin resistance have been reported to exhibit increases in whole-body protein degradation (37,38). Studies using cell lines or isolated primary cells chronically exposed to insulin have revealed that the reduced level of IRS-1 protein is due to enhanced degradation (39). Other studies have demonstrated that a major effect of insulin is regulation of protein degradation mediated by the proteasome (19,20). Based on these reports and from our microarray findings, the next logical step was to evaluate whether the

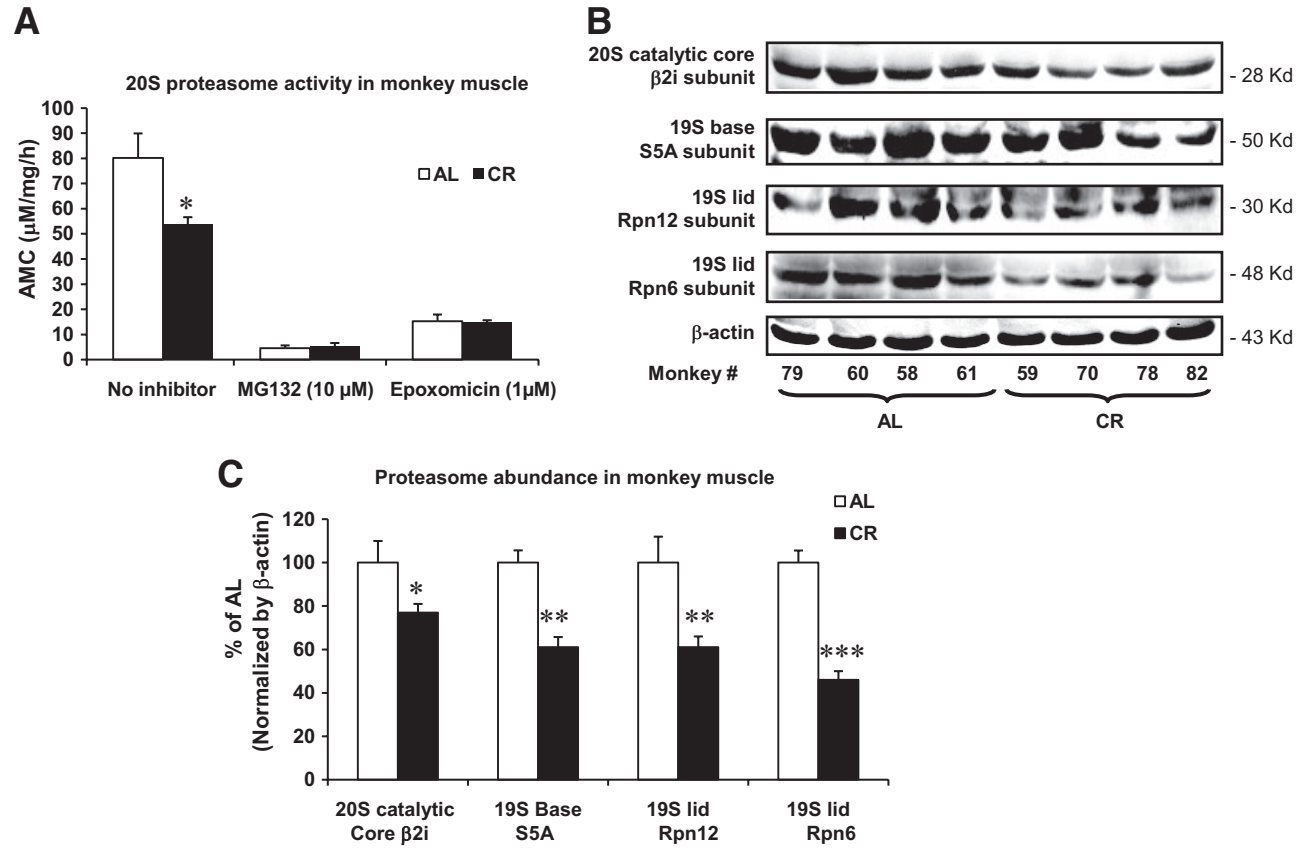

FIG. 7. Abundance of selected 26S proteasome subunits and 20S proteasome activity measurements in the muscle of CR and AL monkeys at the basal time point. *A*: 20S proteasome activity measured in the absence or presence of the proteasome inhibitors MG132 (10 μmol/l) or epoxomicin (1 μmol/l) and performed in duplicate. 20S proteasome activity was measured as the hydrolysis of the fluorogenic peptidyl substrate Suc-LLVY-AMC and is reported as μmol/l AMC per mg protein per h. *B* and *C*: Levels of the 20S proteasome subunit β2i and 19S complex subunits S5A/Rpn10, S9/Rpn6, and S14/Rpn12 in muscle lysate analyzed by Western blot analysis. Data are means ± SEM (n = 13 per group). *P < 0.05, **P < 0.01, and ***P < 0.001 for CR versus AL.

proteins involved in proteasomal degradation are modulated by CR.

Ubiquitin-dependent proteolysis plays an important role in regulating fundamental biological functions, including cell division and cellular differentiation. The proteasome degradation system is composed of two distinct and successive steps: ubiquitin conjugation and proteasome degradation (40). Ubiquitin is first activated by a single ubiquitin-activating enzyme, E1. Following activation, one of several E2 enzymes (ubiquitin-conjugating proteins) transfers ubiquitin from E1 to a member of the ubiquitin-protein ligase family, E3, to which the substrate protein is specifically bound. E3 catalyzes the last step in the conjugation process, covalent attachment of ubiquitin to the substrate (41). Ubiquitin-tagged proteins are then recognized and degraded by the 26S proteasome complex, which consists of the 20S catalytic core complex capped on one or both ends by 19S regulatory complexes (32). In support of the hypothesis that CR may modulate the ubiquitin-proteasome system, transcriptional levels of ubiquitin-specific peptidase 2 and 18 (USP2 and USP18) were reduced. Moreover, skeletal muscle from animals randomized to CR had decreased 20S proteasome activity and greatly reduced protein abundance of selected proteasome subunits. Collectively, our data support the hypothesis that CR enhances the insulin signaling cascade, and one of the contributing mechanisms may be secondary to modulating the ubiquitin-proteasome system in skeletal muscle.

There were other genes of interest that were modulated with CR including those involved in lipid metabolism, e.g., LPL and related enzyme transcriptional levels (Tables 1–3). In addition, we observed significantly increased SIRT1 protein abundance and gene expression with CR in primates. This result appears to be consistent with data found in rodent studies (11,42), but other investigators suggest that the regulation of SIRT1 activity during CR may be tissue specific (43). Thus, the relationship between SIRT1 and insulin signaling in CR animals needs to be further studied.

Our data demonstrating that insulin signaling proteins are increased in muscle with CR appear to be in contrast to many published studies. For example, Gazdag et al. (18) evaluated CR in rhesus monkeys and reported only that the content of IRS-1 approached significance ($P = 0.051$). Friedman et al. (44) reported no change in GLUT4 protein in skeletal muscle but observed a significant improvement in insulin sensitivity in obese human subjects after an average weight loss of 36%. Kim et al. (45) reported improvement in insulin sensitivity with enhanced insulin-stimulated receptor and IRS-1 tyrosine phosphorylation without change in protein content in muscle. Previously, we reported that there was no change in GLUT4 levels for heart or diaphragm muscle between AL or CR animals despite increase in insulin sensitivity (22). Thus, it is important to note that an increase in insulin signaling proteins or GLUT4 abundance does not appear to be essential for increased insulin sensitivity with reduction in caloric intake. Taken together, the mechanism by which CR has its effects on insulin action in cynomolgus monkeys may be different from those reported in other species that demonstrate improved insulin action with CR (i.e., humans, rhesus monkeys, rats, and mice) (1–3,13–18,42). It is not known at this time whether the differences are related to the species, composition of diet, age at CR initiation, length of CR intervention, or other factors.

In summary, our data demonstrate that CR enhances insulin sensitivity and skeletal muscle content of insulin signaling proteins in cynomolgus monkeys. Because ambient protein levels are determined by transcription, mRNA translation, and degradation, any of these processes could have contributed to the observations. However, the data do support the finding that a contributing cellular mechanism by which CR enhances insulin action in vivo may be secondary to modulation of protein degradation via the ubiquitin-proteasome system. The mechanism for the specificity for the sparing of degradation of insulin signaling proteins, but not most proteins, remains unexplained and will need to be confirmed with more precise mechanistic studies.

ACKNOWLEDGMENTS

This study was supported by National Institutes of Health Grants AG010816 and AG000578 (awarded to W.T.C.). This project used Genomics Core facilities that are supported in part by COBRE (NIH P20-RR021945) and CNRU (NIH 1P30-DK072476) center grants from the National Institutes of Health.

No potential conflicts of interest relevant to this article were reported.

We thank Hui Xie for assistance with microarray data analysis and Nicole Mestayer for preparing this article.

REFERENCES

1. Weindruch R. The retardation of aging by caloric restriction: studies in rodents and primates. Toxicol Pathol 1996;24:742–745
2. Goto S, Takahashi R, Radak Z, Sharma R. Beneficial biochemical outcomes of late-onset dietary restriction in rodents. Ann N Y Acad Sci 2007;1100: 431–441
3. Lane MA, Black A, Handy A, Tilmont EM, Ingram DK, Roth GS. Caloric restriction in primates. Ann N Y Acad Sci 2001;928:287–295
4. Dhahbi JM, Kim HJ, Mote PL, Beaver RJ, Spindler SR. Temporal linkage between the phenotypic and genomic response to caloric restriction. Pro Natl Acad Sci U S A 2004;101:5524–5529
5. Merry BJ. Molecular mechanisms linking caloric restriction and longevity. Int J Biochem Cell Biol 2002;34:1340–1354
6. Sohal RS, Weindruch R. Oxidation stress, caloric restriction, and aging. Science 1996;273:59–63
7. Kristal BA, Yu BP. An emerging hypothesis: synergistic induction of aging by free radicals and maillard reactions. J Gerontol 1992;47:B107–B114
8. Walford RL, Spindler SR. The response to calorie restriction in mammals shows features also common to hibernation: a cross-adaptation hypothesis. J Gerontol A Biol Sci Med Sci 1997;52:B179–B183
9. Van Remmen HA, Ruvkun G. Gene expression and protein degradation. In *Handbook of Physiology*. Masoro EJ, Ed. New York, Oxford University Press, 1995, p. 171–234
10. Hursting SD, Lavigne JA, Berrigan D, Perkins SN, Barrett JC. Caloric restriction, aging, and cancer prevention: mechanisms of action and applicability to humans. Annu Rev Med 2003;54:131–152
11. Cohen HY, Miller CM, Bitterman KJ, Wall NR, Hekking B, Kessler B, Howitz KT, Gorospe M, Cabo RD, Sinclair DA. Calorie restriction promotes mammalian cell survival by inducing the SIRT1 deacetylase. Science 2004;305:390–392
12. Kim JE, Chen J, Lou ZK. DBC1 is a negative regulator of SIRT1. Nature 2008;451:583–586
13. Civatarese AE, Carling S, Heilbronn LK, Hulver MH, Ukropcova B, Deutsch WA, Smith SR, Ravussin E; CALERIE Pennington Team. Calorie restriction increases muscle mitochondrial biogenesis in healthy humans. PLoS Med 2007;4:e76
14. Cefalu WT, Wang ZQ, Bell-Farrow AD, Collins J, Morgan T, Wagner JD. Caloric restriction and cardiovascular aging in cynomolgus monkeys (Macaca fascicularis): metabolic, physiologic, and atherosclerotic measures from a 4-year intervention trial. J Gerontol A Biol Sci Med Sci 2004;59:1007–1014
15. Kemnitz JW, Roecker EB, Weindruch R, Elson DF, Baum ST, Bergman RN. Dietary restriction increases insulin sensitivity and lowers blood glucose in rhesus monkeys. Am J Physiol 1994;266:E540–E547

16. Lane NA, Ball SS, Ingram DK, Cutler RG, Eugel J, Read V, Roth GS. Diet restriction in rhesus monkeys lowers fasting and glucose-stimulated glucoregulatory end points. Am J Physiol 1995;268:E941–E948
17. Bodkin NL, Ortmeyer HK, Hansen BC. Long-term dietary restriction in older-aged rhesus monkeys: effects on insulin resistance. J Gerontol A Biol Sci Med Sci 1995;50:B142–B147
18. Gazdag AC, Sullivan S, Kemnitz JW, Cartee GD. Effect of long-term caloric restriction on GLUT4, phosphatidylinositol-3 Kinase p85 subunit, and insulin receptor substrate-1 levels in rhesus monkey skeletal muscle. J Gerontol A Biol Sci Med Sci 2000;55:B44–B46
19. Russell-Jones DL, Umpleby M. Protein anabolic action of insulin, growth hormone and insulin-like growth factor I. Eur J Endocrinol 1996;135:631–642
20. Bennett RG, Hamel FG, Duckworth WC. Insulin inhibits the ubiquitin-dependent degrading activity of the 26S proteasome. Endocrinology 2000; 141:2508–2517
21. Wang X, Hu Z, Hu J, Du J, Mitch WE. Insulin resistance accelerates muscle protein degradation: activation of the ubiquitin-proteasome pathway by defects in muscle cell signaling. Endocrinology 2006;147:4160–4168
22. Wang ZQ, Bell-Farrow AD, Sonntag WE, Cefalu WT. Effect of age and caloric restriction on insulin receptor binding and glucose transporter levels in aging rats. Exp Gerontol 1997;32:671–684
23. Le Marchand-Brustel Y, Gremeaux T, Ballotti R, Van Obberghen E. Insulin receptor tyrosine kinase is defective in skeletal muscle of insulin-resistant obese mice. Nature 1985;315:676–679
24. Zhao WQ, De Felice FG, Fernandez S, Chen H, Lambert MP, Quon MJ, Grant A, Krafft GA, Klein WL. Amyloid β oligomers induce impairment of neuronal insulin receptors. FASEB J 2008;22:246–260
25. Wang ZQ, Zhang XH, Russell JC, Hulver M, Cefalu WT. Chromium picolinate enhances skeletal muscle cellular insulin signaling in vivo in obese, insulin-resistant JCR:LA-cp rats. J Nutr 2006;136:415–420
26. Corbould A. Chronic testosterone treatment induces selective insulin resistance in subcutaneous adipocytes of women. J Endocrinol 2007;192: 585–594
27. Goodyear LJ, Giorgino F, Sherman LA, Carey J, Smith RJ, Dohm GL. Insulin receptor phosphorylation, insulin receptor substrate-1 phosphorylation, and phosphatidylinositol 3-kinase activity are decreased in intact skeletal muscle strips from obese subjects. J Clin Invest 1995;95:2195–2204
28. Walker SJ, Wang Y, Grant KA, Chan F, Hellmann GM. Long versus short oligonucleotide microarrays for the study of gene expression in nonhuman primates. J Neurosci Methods 2006;152:179–189
29. Meng L, Mohan R, Kwok BH, Elofsson M, Sin N, Crews C. Epoxomicin, a potent and selective proteasome inhibitor, exhibits *in vivo* antiinflammatory activity. Proc Natl Acad Sci U S A 1999;96:10403–10408
30. Bolstad BM, Irizarry RA, Astrand M, Speed TP. A comparison of normalization methods for high density oligonucleotide array data based on variance and bias. Bioinformatics 2003;19:185–193
31. Eisen MB, Spellman PT, Brown PO, Botstein D. Cluster analysis and display of genome-wide expression patterns. Proc Natl Acad Sci U S A 1998;95:14863–14868
32. Voges D, Zwickl P, Baumeister W. The 26S proteasome: a molecular machine designed for controlled proteolysis. Annu Rev Biochem 1999;68: 1015–1068
33. Zhu M, Cabo RD, Lane MA, Ingram DK. Caloric restriction modulates early events in insulin signaling in liver and skeletal muscle of rat. Ann N Y Acad Sci 2004;1019:448–452
34. Masternak MM, Al-Regaiey KA, Del Rosario Lim MM, Jimenez-Ortega V, Panici JA, Bonkowski MS, Kopchick JJ, Wang Z, Bartke A. Caloric restriction and growth hormone receptor knockout: effects on expression of genes involved in insulin action in the heart. Exp Gerontol 2006;41:417–429
35. Kayo T, Allison DB, Weindruch R, Prolla TA. Influences of aging and caloric restriction on the transcriptional profile of skeletal muscle from rhesus monkeys. Proc Natl Acad Sci U S A 2001;98:5093–5098
36. Kasinath BS, Mariappan MM, Sataranatarajan K, Lee MJ, Feliers K. mRNA translation: unexplored territory in renal science. J Am Soc Nephrol 2006;17:3281–3292
37. Lee AV, Gooch JL, Oesterreich S, Guler RL, Yee D. Insulin-like growth factor I-induced degradation of insulin receptor substrate 1 is mediated by the 26S proteasome and blocked by phosphatidylinositol 3-kinase inhibition. Mol Cell Biol 2000;20:1489–1496
38. Sun XJ, Goldberg JL, Qiao LY, Mitchell JJ. Insulin-induced insulin receptor substrate-1 degradation is mediated by the proteasome degradation pathway. Diabetes 1999;48:1359–1364
39. Rice KM, Turnbow MA, Garner CW. Insulin stimulates the degradation of IRS-1 in 3T3–L1 adipocytes. Biochem Biophys Res Commun 1993;190:961–967
40. Ciechanover A. The ubiquitin-proteasome pathway: on protein death and cell life. EMBO J 1998;17:7151–7160
41. Kornitzer D, Ciechanover A. Modes of regulation of ubiquitin-mediated protein degradation. J Cell Physiol 2000;182:1–11
42. Masoro EJ. Role of sirtuin proteins in life extension by caloric restriction. Mech Ageing Dev 2004;125:591–594
43. Chen D, Bruno J, Easlon E, Lin S-J, Cheng H-L, Alt FW, Guarente L. Tissue-specific regulation of SIRT1 by calorie restriction. Genes Dev 2008;22:1753–1757
44. Friedman JE, Dohm GL, Leggett-Frazier N, Elton CW, Tapscott EB, Pories WP, Caro JF. Restoration of insulin responsiveness in skeletal muscle of morbidly obese patients after weight loss. Effect on muscle glucose transport and glucose transporter GLUT4. J Clin Invest 1992;89:701–705
45. Kim YB, Kotani K, Ciaraldi TP, Henry RR, Kahn BB. Insulin-stimulated protein kinase C λ/æ activity is reduced in skeletal muscle of humans with obesity and type 2 diabetes: reversal with weight reduction. Diabetes 2003;52:1935–1942